Symmetry energy in holographic QCD

Lorenzo Bartolini,[a] **Sven Bjarke Gudnason**[a,1]

[a] *Institute of Contemporary Mathematics, School of Mathematics and Statistics, Henan University, Kaifeng, Henan 475004, P. R. China*

E-mail: lorenzo@henu.edu.cn, gudnason@henu.edu.cn

Abstract: We study the symmetry energy (SE), an important quantity in nuclear physics, in the Witten-Sakai-Sugimoto model and in a much simpler hard-wall model of holographic QCD. The SE is the energy contribution to the nucleus due to having an unequal number of neutrons and protons. Using a homogeneous Ansatz representing smeared instantons and quantizing their isospin, we extract the SE and the proton fraction assuming charge neutrality and beta-equilibrium, using quantization of the isospin zeromode. We also show the equivalence between our method adapted from solitons and the usual way of the isospin controlled by a chemical potential at the holographic boundary. We find that the SE can be well described in our models if we allow for a larger 't Hooft coupling than is normally used in phenomenological fits, passing all experimental constraints and is compatible with results from nuclear physics at low densities.

[1] Corresponding author

Contents

1 Introduction 1

2 Model 3

3 Time-dependent configurations 5

4 Symmetry energy 8

5 Proton fraction 10

6 Discussion 12

A Equivalence between rotation in SU(2) and external isospin chemical potential 13

B Isospin density from holographic current 14

1 Introduction

The equation of state (EOS) in nuclear physics is central to nuclear physics from neutron stars to heavy ion collisions, and an important feature is the symmetry energy (SE) as a function of the density. The symmetry energy is the symmetric increase in energy as one moves away from the isospin symmetric point, that is, the point where the number of protons equals that of neutrons, i.e. $E(\rho) = E_0(\rho) + S(\rho)\beta^2 + \cdots$, with $\beta = \frac{N-Z}{A}$ being the difference between the number neutrons N and number of protons Z, normalized by the atomic mass number, $A = Z + N$ — for a nice review see ref. [1]. The symmetry energy is experimentally well constrained around saturation density, $\rho_0 \sim 0.16\text{fm}^{-3}$, to be near $S(\rho_0) \sim 30$ MeV – both from astrophysical observations as well as heavy ion collision data – but much less so at larger densities. The symmetry energy around saturation density is conventionally expanded as

$$S(\rho) = S_0 + \frac{1}{3}L\epsilon + \frac{1}{18}K_{\text{sym}}\epsilon^2 + \cdots \tag{1.1}$$

with $\epsilon := (\rho - \rho_0)/\rho_0$, whereas L and K_{sym} are proportional to the slope and second derivative of the SE with respect to the density. Expectedly, the constraints on L and K_{sym} are less tight than those on S_0. Traditionally, the symmetry energy was defined for nuclear matter, which can be thought of as an infinitely large nucleus at density ρ, and so surface effects are absent. The symmetry energy can equally well be defined for a fixed, but finite, atomic number A.

Current experimental bounds on the first 3 observables of the symmetry energy as in the expansion of the density come from mass, radius and tidal deformation of neutron

stars, excitation energies of isobaric analog states, neutron skin in Sn isotopes and ^{208}Pb as well as heavy ion collision data [2–6, 5, 7–9].

The equation of state in nuclear physics relates the energy density with the pressure and is the main ingredient in the understanding of neutron stars as well as heavy ion collisions. The problem with obtaining the equation of state for nuclei is that the strong nuclear force is governed by Quantum Chromodynamics (QCD), an inherently strongly coupled theory and hence cannot be tackled by perturbation theory or first-principles calculations. Nuclear physics, in particular, ab initio methods, like the no-core shell model [10], utilize pion scattering data to reconstruct the interaction potential of nuclei and this approach leads to solid predictions for the interaction potential and the chiral effective field theory can accurately determine the EOS [11], albeit only at relatively small densities. QCD at high energies is perturbative due to its asymptotically free nature, and hence can be used to make solid predictions for the EOS [12], unfortunately at pressures far larger than those of a neutron star – the most compact object known, not collapsed into a black hole (BH).

A new paradigm of studying QCD and attempting to extract observables for nuclear physics and hadronic physics, was envisioned by Maldacena at the end of the '90-ies [13] and further elaborated by Witten [14]. After a couple of decades, the mentioned framework known as holography or AdS/CFT, has been coined holographic QCD (HQCD) when applied to the strong nuclear force [15–17]. There are two main approaches to HQCD, top-down and bottom-up; the top-down approach is based on string-theory constructions and the most prominent example is the Witten-Sakai-Sugimoto model (WSS) [14, 18, 19]. For the bottom-up construction, which shares similar theoretical ingredients, two main types of models are known as soft-wall (SW) (e.g. Improved HQCD [20, 21] and V-QCD [22–24]) and hard-wall (HW) models [25–33]. Especially, the top-down type of HQCD have quite some predictive power, in the sense that the models have very few adjustable parameters [15–17]. For the WSS, there is the mass scale and the 't Hooft coupling, where the mass scale is normally fitted to the mass of the ρ meson and the 't Hooft coupling is determined from the pion decay constant [18].

Attempts have already been made at extracting the SE from various HQCD models, including top-down approaches as in the D4/D6 model [34] and even the WSS model, see ref. [35], and NSs have been constructed using the holographically extracted EOS to solve the governing Tolman-Oppenheimer-Volkov (TOV) equations [36, 37]. The SE, however, comes out too large in the WSS [35]. In HQCD in contrast to traditional nuclear physics, the proton and the neutron are not point particles, but are described by a topological soliton, the Sakai-Sugimoto soliton [18, 38–40], which is initially isospin symmetric – that is, the proton is equal to the neutron. In order to compute the SE, we must distinguish the proton from the neutron and this can be done by the introduction of an isospin chemical potential [35].

In this paper, we propose using the homogeneous Ansatz in the WSS, but quantizing the isospin symmetry – a technique known from the Skyrme model [41–43], which is the leading-order low-energy effective theory of the WSS model [18]. The quantization of the isospin symmetry introduces the isospin quantum number, which makes it possible to extract the SE as the coefficient of the square of the difference between the number of protons and neutrons. The quantization method of introducing isospin is also shown to

be equivalent to using a chemical potential, see app. A. We find a lower SE compared to previous attempts in the WSS and in particular, we find a phenomenologically viable value of the constant $S(\rho_0)$ at saturation density and the first two coefficients L and $K_{\rm sym}$ are compatible with current experimental bounds from astrophysics and heavy ion collision data for certain choices of model parameters.

2 Model

We will treat the WSS and the HW model on equal footing in the following. The model at low energies is described by the Yang-Mills (YM) and Chern-Simons (CS) actions in 5-dimensional AdS_5 spacetime (M, g):

$$\begin{aligned} S_{\rm YM} &= -\kappa \,\mathrm{Tr} \int_M \mathcal{F} \wedge *\mathcal{F}, \\ S_{\rm CS} &= \frac{N_c}{24\pi^2} \,\mathrm{Tr} \int_M \left[\mathcal{A} \wedge \mathcal{F}^2 - \frac{\mathrm{i}}{2} \mathcal{A}^3 \wedge \mathcal{F} + \frac{1}{10} \mathcal{A}^5 \right], \end{aligned} \tag{2.1}$$

with $S = S_{\rm YM} + S_{\rm CS}$ being the total action, the constant $\kappa = \frac{\lambda N_c}{216\pi^3}$ for the WSS model and $\kappa = M_5$ for the HW model, $\lambda = g_{\rm YM}^2 N_c$ the 't Hooft coupling, N_c the number of colors of QCD (i.e. 3 in nature), the field strength 2-form is

$$\mathcal{F} = \tfrac{1}{2}(\partial_\alpha \mathcal{A}_\beta - \partial_\beta \mathcal{A}_\alpha + \mathrm{i}[\mathcal{A}_\alpha, \mathcal{A}_\beta]) \mathrm{d}x^\alpha \wedge \mathrm{d}x^\beta, \tag{2.2}$$

$\alpha, \beta = 0, 1, 2, 3, 4$ with $x^4 = z$ the holographic coordinate, and the power of forms is understood with the wedge product. The metric is

$$g = h(z)k(z)(\mathrm{d}x^\mu)^2 + h^2(z)\mathrm{d}z^2, \tag{2.3}$$

with $h(z) = k^{-1/3}(z) = (1 + z^2)^{-1/3}$, $z \in (-\infty, \infty)$ for WSS and $h(z) = k(z) = \mathsf{L}/z$, $z \in [0, \mathsf{L}]$ for the HW model, and the index $\mu = 0, 1, 2, 3$ is summed over in the metric.

The gauge field can be decomposed for future convenience in the Abelian and non-Abelian parts as

$$\mathcal{A}_\alpha = A^a_\alpha T^a + \widehat{A}_\alpha \frac{\mathbb{1}}{2}, \tag{2.4}$$

where the generators of SU(2) T^a are chosen as $T^a = \frac{1}{2}\tau^a$ so that $\mathrm{Tr}\, T^a T^b = \frac{1}{2}\delta^{ab}$, and the space-time indices follow the convention:

$$\alpha, \beta, \ldots = \{0, M\}; \quad M, N, \ldots = \{i, z\}; \quad \mu, \nu, \ldots = \{0, i\}. \tag{2.5}$$

In writing eq. (2.1), we performed dimensional reduction in the WSS, integrating out S^4 from the original nine-dimensional action for the stack of $D8-$Branes, while in the HW we set the scalar field to zero, which is appropriate in the homogeneous baryonic phase, following ref. [37].

Two further steps were employed in order to write the action and equations of motion for the two models in a compact way. For the HW model we assumed the symmetry properties for the fundamental fields $\mathcal{L}_M, \mathcal{R}_M$ as follows:

$$\mathcal{L}_i = -\mathcal{R}_i, \qquad \mathcal{L}_0 = \mathcal{R}_0. \tag{2.6}$$

For the WSS model, we similarly assumed parity properties of the fields with respect to z:

$$\mathcal{A}_i(z) = -\mathcal{A}_i(-z), \qquad \mathcal{A}_0(z) = +\mathcal{A}_0(-z). \tag{2.7}$$

With these procedures, we halve the number of fields in the HW model (from $\mathcal{L}, \mathcal{R}$ to $\mathcal{A}$) and the integration interval in the WSS model (from $(-\infty, +\infty)$ to $[0, +\infty)$) generating an overall factor of 2 in the action in both cases.

As a last step, we introduce generic symbols $z_{\rm IR}, z_{\rm UV}$ to indicate the infrared and ultraviolet boundary values of the holographic coordinate[1], which in the two models assume the values

$$z_{\rm IR} = \begin{cases} 0 & \text{WSS} \\ \mathsf{L} & \text{HW} \end{cases}, \qquad z_{\rm UV} = \begin{cases} +\infty & \text{WSS} \\ 0 & \text{HW} \end{cases}. \tag{2.8}$$

The classical homogeneous Ansatz for isospin-symmetric matter, reasonable for large-density computations, is defined as

$$\mathcal{A}_0^{\rm cl} = \tfrac{1}{2}\widehat{a}_0, \quad \mathcal{A}_i^{\rm cl} = -\tfrac{1}{2}H\tau^i, \quad \mathcal{A}_z^{\rm cl} = 0, \tag{2.9}$$

where $\{\widehat{a}_0, H\} = \{\widehat{a}_0, H\}(z)$ are functions of the holographic coordinate z. We have suppressed the unit 2-by-2 matrices in the terms without a Pauli matrix $\boldsymbol{\tau}$.

The function $H(z)$ encodes the baryonic density through its value at $z = z_{\rm IR}$: if either $H(z_{\rm IR})$ or $H'(z_{\rm IR})$ vanish, then the baryon number would also vanish, so we will assume that $H(z)$ obeys a Dirichlet boundary condition $H(z_{\rm IR}) = H_0$, with the value of H_0 to be determined by minimization of the action. This defines the baryon density ρ (assuming $H(z) \to 0$ for $z \to z_{\rm UV}$) as follows:

$$\begin{aligned} \rho &= \frac{1}{16\pi^2}\int {\rm d}z\, \epsilon^{MNPQ}\, {\rm Tr}\, F_{MN}F_{PQ} \\ &= -\frac{3}{4\pi^2}\int {\rm d}z\, H'H^2 \\ &= -\epsilon\frac{1}{4\pi^2}\left[H^3\right]_{z_{\rm IR}}^{z_{\rm UV}}, \end{aligned} \tag{2.10}$$

so that the infrared boundary condition for the numerical integration of the function $H(z)$ is directly related to the baryon number density as:

$$H(z_{IR}) = \epsilon\left(4\pi^2\rho\right)^{\frac{1}{3}}, \tag{2.11}$$

where for convenience of putting the two models on same footing, have defined the integral in the holographic direction as

$$\int {\rm d}z\, f(z) := \epsilon\int_{z_{\rm IR}}^{z_{\rm UV}} {\rm d}z\, f(z), \tag{2.12}$$

[1] In the WSS model, the spatial manifold only has a UV boundary at $z = \pm\infty$. However, when we introduced the "folding" of the coordinate z exploiting the assumptions (2.7), we effectively introduced an IR boundary at the folding point $z_{\rm IR} = 0$. Moreover, the homogeneous Ansatz will introduce a discontinuity in the field A_i at that point.

which we will use throughout the paper and ϵ assumes different is the sign depending on the model:

$$\epsilon = \begin{cases} +1 & \text{WSS} \\ -1 & \text{HW} \end{cases} \tag{2.13}$$

Thus the integral is defined in such a way to take into account the different orientation in the integration along z, dictated by the choice of coordinates for the two models. Note that this choice of boundary condition for $H(z_{\rm IR})$ means that in the WSS, once we restore the full domain of integration $z \in (-\infty, = \infty)$, the function $H(z)$ will be discontinuous. This still leads to a continuous field strength, since both H' and H^2 are continuous functions. For the HW model instead, this choice just means that we cannot enforce the standard boundary condition $L_\mu(z_{\rm IR}) - R_\mu(z_{\rm IR}) = 0$, which has to be replaced with the one above, implying $L_\mu(z_{\rm IR}) = -R_\mu(z_{\rm IR})$.

3 Time-dependent configurations

We wish to include the effects of isospin asymmetry in the system. To do so, we follow a method inspired by the single-soliton analysis: we know that for the single baryon, the proton and the neutron are described as degenerate (in absence of quark mass terms[2]) quantum states of the effective Hamiltonian obtained by considering a slow rotation in SU(2). The homogeneous Ansatz shares a similar structure with the single-soliton configuration, made easier by the absence of translational moduli[3] X_M and ρ (but with the minor complication of not having an analytical configuration to approximate our static Ansatz (2.9)), so we can attempt to follow steps similar to the ones in refs. [38] and [39], in order to obtain a time-dependent configuration – yet to be quantized.

We start by assuming a configuration of the form

$$A_0 = 0, \tag{3.1}$$
$$A_i = V A_i^{\rm cl} V^{-1} - {\rm i} V \partial_i V^{-1}, \tag{3.2}$$
$$A_z = -{\rm i} V \partial_z V^{-1}, \tag{3.3}$$

which implies the following transformations in the field strenghts:

$$F_{MN} = V F_{MN}^{\rm cl} V^{-1}, \tag{3.4}$$
$$F_{0z} = -V D_z^{\rm cl} \Phi V^{-1}, \tag{3.5}$$
$$F_{0i} = 0, \tag{3.6}$$

[2]See ref. [44] for the effect of breaking the degeneracy for the WSS model, when including the quark mass terms.

[3]The translational moduli X_i are absent because of the assumption of homogeneity, while the pseudo-modulus size ρ is fixed by the numerical solution as to minimize energy. The pseudo-modulus Z describing the center of the soliton in z is fixed by our Ansatz to be at the position of the discontinuity. This in principle can also be determined by choosing $Z = z_0$ that minimzes the free energy as opposed to our simpler choice $z_0 = 0$ for all densities. See ref. [45] for the inclusion of this effect in the static approximation.

where $V(z,t)$ encodes the time-dependent rotation in SU(2), and Φ is defined as

$$\Phi \equiv -\mathrm{i}V^{-1}\dot{V}. \tag{3.7}$$

Notice, this is not a gauge transformation since the field A_0 is not transformed along with the rest. The function $V(z,t)$ needs to depend on z in order to allow us to satisfy the equation of motion

$$-\kappa\left(h(z)D_jF^{0j} + D_z\left(k(z)F^{0z}\right)\right) + \frac{N_c}{64\pi^2}\epsilon^{0\alpha_1\alpha_2\alpha_3\alpha_4}F_{\alpha_1\alpha_2}\widehat{F}_{\alpha_3\alpha_4} = 0. \tag{3.8}$$

The function $V(z,t)$ is holographically dual to the SU(2)-valued collective coordinate $a(t)$, as we choose it such that

$$V(z \to z_{\mathrm{UV}}, t) = a(t), \tag{3.9}$$

which in turn implies

$$\Phi(z \to z_{\mathrm{UV}}, t) = -\mathrm{i}a^{-1}\dot{a} \equiv \frac{1}{2}\boldsymbol{\chi}\cdot\boldsymbol{\tau}, \tag{3.10}$$

where $\boldsymbol{\chi}$ is the boundary angular velocity. The presence of a nonvanishing F_{0z} will also enable a source term for the fields $\widehat{A}_i$ via the Chern-Simons action, so we will have to complete the field content by turning on $\widehat{A}_i = -\frac{1}{2}L\chi^i$: here we already guessed that the vector field will be proportional to the angular velocity χ^i, and we can do so without loss of generality, since in the homogeneous case this is the only three-vector available to the Abelian field.

At this stage the problem is well posed and the function $\Phi(z,t)$ can be found by solving eq. (3.8), but it is more convenient to perform a gauge transformation to make the system easier to treat.

We perform the gauge SU(2) transformation

$$A_\alpha \to A^S_\alpha = GA_\alpha G^{-1} - \mathrm{i}G\partial_\alpha G^{-1}, \qquad G \equiv aV^{-1}, \qquad \alpha = 0,1,2,3,4, \tag{3.11}$$

where the superscript "S" stands for "singular", because this is reminiscent of the transformation changing from the regular gauge to the singular gauge in the single-soliton case. With this choice (dropping the superscript "S" for convenience, since we will use this gauge henceforth) the field content becomes

$$A_0 = a\left(\Phi - \frac{1}{2}\boldsymbol{\tau}\cdot\boldsymbol{\chi}\right)a^{-1}, \tag{3.12}$$

$$A_i = aA_i^{\mathrm{cl}}a, \tag{3.13}$$

$$A_z = 0. \tag{3.14}$$

Now we can factorize the function $\Phi(z,t)$ as

$$\Phi = \Phi^a\chi^a \equiv \widetilde{G}\boldsymbol{\chi}\cdot\boldsymbol{\tau}, \tag{3.15}$$

and since we imposed eq. (3.10), we see that

$$\widetilde{G}(z \to z_{\mathrm{UV}}) = \frac{1}{2}. \tag{3.16}$$

We then conclude that the field A_0 in this gauge vanishes at the UV boundary, and can be expressed as

$$A_0 = G(z) a \boldsymbol{\chi} \cdot \boldsymbol{\tau} a^{-1}, \qquad G(z \to z_{\rm UV}) = 0. \tag{3.17}$$

We notice that this result is exactly what one would expect by allowing for the most general field configuration respecting spherical symmetry, homogeneity in three-dimensional flat space, and the gauge choice $A_z = 0$. Taking the functions $H, \widehat{a}_0, G, L$ to be independent of $\boldsymbol{\chi}$ amounts to considering a slow rotation, thus including only linear terms in $\boldsymbol{\chi}$ in the Ansatz.

Whereas $\frac{1}{2}\boldsymbol{\chi} \cdot \boldsymbol{\tau}$ is the matrix form of the boundary angular velocity, $\frac{1}{2} a \boldsymbol{\chi} \cdot \boldsymbol{\tau} a^{-1} = -\mathrm{i} \dot{a} a^{-1}$ is the matrix form of the boundary angular isospin velocity (i.e. describing rotations in SU(2) instead of in space). Thus, although one may think we are spinning the fields in space, this is really an isospin action on the homogeneous fields.

The final form of our time-dependent homogeneous Ansatz is then summarized in compact notation as:

$$\mathcal{A}_0 = G a \boldsymbol{\chi} \cdot \boldsymbol{\tau} a^{-1} + \tfrac{1}{2}\widehat{a}_0, \quad \mathcal{A}_i = -\tfrac{1}{2}\left(H a \tau^i a^{-1} + L \chi^i\right), \quad \mathcal{A}_z = 0, \tag{3.18}$$

with the mandatory boundary condition $G(z \to z_{\rm UV}) = 0$.

This Ansatz leads to the action

$$\begin{aligned} S_{\rm YM} = -\kappa \int \mathrm{d}^4 x \int \mathrm{d}z \Big[& -8hH^2 \left(G + \frac{1}{2}\right)^2 \chi \cdot \chi + 3hH^4 \\ & + k\left[(L')^2 - 4(G')^2 + 8(KH)^2\right] \chi \cdot \chi + 3k(H')^2 - k(\hat{a}_0')^2 \Big], \end{aligned} \tag{3.19}$$

$$S_{\rm CS} = -\frac{N_c}{8\pi^2} \int \mathrm{d}^4 x \int \mathrm{d}z \; \hat{a}_0 H' H^2 + \frac{N_c}{4\pi^2} \int \mathrm{d}^4 x \int \mathrm{d}z \left(LH' - L'GH\right) H \chi \cdot \chi, \tag{3.20}$$

which gives rise to the equations of motion

$$hH^3 - \frac{1}{2}\partial_z(kH') - \frac{N_c}{32\pi^2\kappa} H^2 \hat{a}_0' = 0, \tag{3.21}$$

$$\partial_z(k\hat{a}_0') + \frac{3N_c}{16\pi^2} H^2 H' = 0, \tag{3.22}$$

$$\partial_z(kG') - hH^2(1+2G) + \frac{N_c}{32\pi^2\kappa} H^2 L' = 0, \tag{3.23}$$

$$\partial_z(kL') + \frac{N_c}{8\pi^2\kappa} H \left[HG' + (1+2G)H'\right] = 0, \tag{3.24}$$

where the first two equations of motion are truncated to order $\boldsymbol{\chi}^0$, whereas the latter two only appear at quadratic order in $\boldsymbol{\chi}$. Including the subleading $\boldsymbol{\chi}^2$ corrections to the solutions of H and $\widehat{a}_0$ has a negligible impact, which we checked explicitly.

This set of equations is composed by ODEs in the holographic coordinate z and can be solved with standard off-the-peg solvers in packages like Mathematica or Matlab, once we specify all the boundary conditions:

$$G'(z_{\rm IR}) = \widehat{a}_0'(z_{\rm IR}) = L(z_{\rm IR}) = 0, \quad H(z_{\rm IR}) = \epsilon(4\pi^2\rho)^{\frac{1}{3}}, \tag{3.25}$$

and all fields are vanishing at $z = z_{\rm UV}$. We recall that that in the chosen coordinates $z_{\rm IR} = 0$ ($z_{\rm IR} = \mathsf{L}$), $z_{\rm UV} = \infty$ ($z_{\rm UV} = 0$) and $\epsilon = +1$ ($\epsilon = -1$) for the WSS (HW) model.

Another possible approach would be to keep the fields in a static configuration, hence keeping the freedom to set the standard orientation of eq. (2.9), and introduce an external isospin chemical potential, which holographically amounts to introducing a finite UV boundary value for the field A_0 [35, 46]: in app. A we show that this approach is related to ours by a gauge transformation, hence leading to the same physics.

4 Symmetry energy

The terms quadratic in $\boldsymbol{\chi}$ exactly produce the SE upon Hamiltonian quantization:

$$\begin{aligned} H &= \frac{1}{2} V\Lambda \boldsymbol{\chi}\cdot\boldsymbol{\chi} + VU \\ &= 2V\Lambda \dot{a}_m^2 + VU \\ &= \frac{\pi_m^2}{8V\Lambda} + VU \\ &= \frac{I(I+1)}{2V\Lambda} + VU, \end{aligned} \tag{4.1}$$

where canonical quantization of a_m, $m = 0, 1, 2, 3$, a coordinate on the 3-sphere ($a_m^2 = 1$), leads to the momentum conjugate

$$\pi_m = \frac{\partial H}{\partial \dot{a}_m} = 4V\Lambda \dot{a}_m, \tag{4.2}$$

and hence to $\pi_m^2 = \ell(\ell+2)$ being the spherical harmonics and $\ell = 2I$, with I the isospin quantum number [41][4]. The identification of $V\boldsymbol{\chi}^2$ and $I(I+1)/V$ coming from Hamiltonian quantization is also justified by the holographic dictionary, since it can be obtained by computing the third component of the isovector charge density, see app. B for a detailed computation. The functionals Λ and U are defined as

$$\begin{aligned} \Lambda &= 2\kappa \int \mathrm{d}z \left[2hH^2(2G+1)^2 + k((L')^2 + 4(G')^2)\right], \\ U &= \kappa \int \mathrm{d}z \left[3hH^4 + 3k(H')^2 + k(\widehat{a}_0')^2\right], \end{aligned} \tag{4.3}$$

where V denotes the spatial 3-volume. Using now the relation between isospin and the number of protons and neutrons:

$$2I = Z - N = -\beta A, \tag{4.4}$$

with Z the proton number and N the neutron number, as well as the atomic number

$$A = Z + N = V\rho, \tag{4.5}$$

[4] Due to the simplicity of the homogeneous Ansatz, the isospin quantum number is identical to the spin quantum number in magnitude; this is an artifact of the Ansatz, but it does not increase the kinetic energy. In particular, for reading off the coefficient of the symmetry at $\beta = 0$, this artifact of the approximation of using the homogeneous Ansatz is irrelevant.

being the product of the 3-volume and the baryonic density. β is defined as the normalized difference between the number of neutrons and protons, $\beta = (N - Z)/A$, hence we have

$$\frac{H}{A} = \frac{U}{\rho} + S(\rho)\beta^2 + \mathcal{O}(V^{-1}), \tag{4.6}$$

$$S(\rho) = \frac{\rho}{8\Lambda}, \tag{4.7}$$

where $S(\rho)$ is the symmetry energy as a function of the density.

Using the standard phenomenological fit for the WSS model of ref. [19], we set $\lambda = 16.63$ and find the first SE expansion parameters as

$$\frac{S_0}{M_{\rm KK}} = 0.1032, \qquad \frac{L}{M_{\rm KK}} = 0.1339, \qquad \frac{K_{\rm sym}}{M_{\rm KK}} = -0.1982, \tag{4.8}$$

where the Kaluza-Klein scale only enters as an overall factor. Using the standard fit [19], $M_{\rm KK} = 949$MeV, we obtain $S_0 = 97.95$MeV, $L = 136.2$MeV, and $K_{\rm sym} = -188.1$MeV, which are somewhat larger than values typically obtained from phenomenological models [1], but much smaller than obtained in the WSS previously [35]. For the HW model, we fix $M_5 = \frac{N_c}{12\pi^2}$ using the leading OPE coefficient of the vector current correlator [30], for which the first few SE expansion parameters are

$$S_0\mathsf{L} = 0.2743, \quad L\mathsf{L} = 0.3905, \quad K_{\rm sym}\mathsf{L} = 1.347, \tag{4.9}$$

where L^{-1} is the mass scale of the HW model, which we set as $\mathsf{L}^{-1} = 150$MeV following ref. [37], which provides phenomenologically good results for neutron stars in terms of mass-radius data; this yields $S_0 = 41.13$MeV, $L = 58.57$MeV, and $K_{\rm sym} = 202.1$MeV. The SE at saturation density and the slope are in fairly good agreement with phenomenological constraints, whereas $K_{\rm sym}$ has the opposite sign to most predictions in the literature [1]. The saturation density, ρ_0, in HQCD is defined to be at the onset of baryonic matter, obtained by minimization of the free energy with the baryonic chemical potential as the boundary condition $\widehat{a}_0(z_{\rm UV}) = \mu_B$. The value of ρ_0 obtained this way in the WSS model turns out to be too large by a factor of 3 wrt. nature, an overestimate by the same order of other baryonic quantities.

We explore a larger range of densities for both the WSS and the HW model in Fig. 1a). For the WSS model, we have used the phenomenological value of the 't Hooft coupling ($\lambda = 16.63$) and shown the range of $M_{\rm KK} \in [300, 1200]$MeV with a red shaded area, which includes $M_{\rm KK} = 949$MeV [19] (red solid line), whereas for the HW model the range of $\mathsf{L}^{-1} \in [110, 320]$MeV is shown with a green shaded area, which includes $\mathsf{L}^{-1} = 150$MeV (green solid line) that is chosen from neutron star phenomenology [37] and the highest mass scale is from meson physics [47, 31]. Up-to-date constraints from astrophysics and heavy-ion collision data are shown with grey and cyan shaded areas near and above saturation density and constraints using nuclear excitation energies from isobaric analog states (IAS) are shown with a purple shaded area below saturation density. As can be seen from the figure, the phenomenologically fitted value of the mass scale $M_{\rm KK}$ at 949MeV [38] overestimates the SE with about a factor of 3; however, the fit is made using mesonic observables and is known to overestimate baryonic observables; for instance, the baryon mass is typically overestimated by a factor of 1.7-1.8 [38, 48, 49] using the mesonic fit.

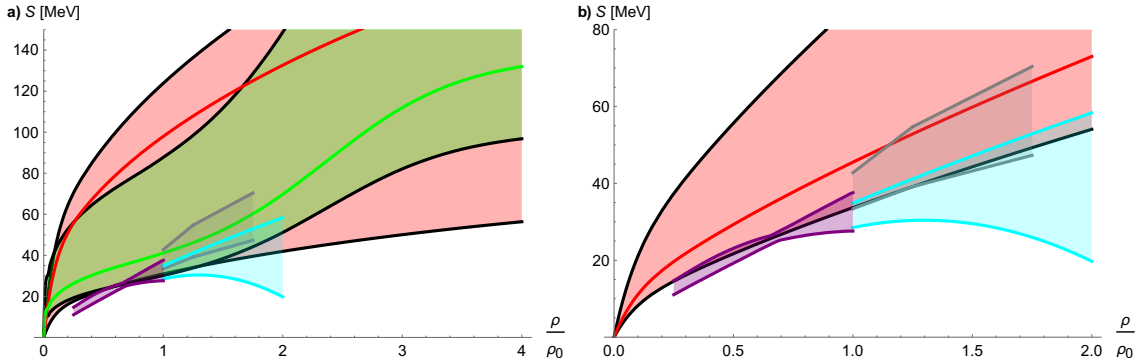

Figure 1. The symmetry energy (SE) calculated in the WSS model with the phenomenological value of the 't Hooft coupling and in the HW model, both using quantization of isospin as functions of the density. a) The red area corresponds to the WSS model with $M_{\rm KK}$ ranging from 300MeV to 1200MeV and the red line in the middle is at 949MeV. The green area corresponds to the HW model with L^{-1} ranging from 110MeV to 320MeV and the green line in the middle is at 150MeV. The constraints from the PREX-II experiment using the neutron skin thickness of ^{208}Pb [6] are shown with a gray shaded area, while the extensive 2021 survey of constraints on the symmetry energy of Li et.al. [4] using neutron stars, are shown with a cyan shaded area. Constraints from isobaric analog states below saturation density are shown with a purple shaded area [2]. b) The SE calculated in the WSS model with the 't Hooft coupling $\lambda = 60$. The red shaded area corresponds to $M_{\rm KK} \in [370, 949]$MeV and the red solid curve is the rescaled phenomenological mass scale, that keeps the pion decay constant at 93MeV.

Although both models come in the ball park of the experimental constraints above saturation density and nuclear physics predictions below saturation density, the shape of the SE does not quite satisfy all the constraints. In the WSS model, however, we can dial the 't Hooft coupling to see whether we can fit in the allowed regions and indeed it is possible by raising both the 't Hooft coupling from the phenomenological value to $\lambda = 60$, as well as the (lower) KK scale from 300MeV to 370MeV, see Fig. 1b). With the larger 't Hooft coupling, the SE of the WSS has a compatible shape to pass all the constraints, but the ρ meson is too light and the baryon mass is too heavy – often a problem in HQCD; the baryon mass is reduced from about 1600MeV to 1191MeV. If we keep the pion decay constant at its phenomenological value, the KK scale, however, is lowered and is shown in Fig. 1b) with a solid red curve – not too far from a the viable solution. The dependence on the 't Hooft coupling for the WSS model is shown in Fig. 2 for the KK scale in the interval 300-1200MeV at saturation density.

5 Proton fraction

We will now consider the proton fraction at β-equilibrium with charged leptons, imposing charge neutrality. Using the Gell-Mann-Nishijima formula, we can relate the baryon density, ρ, and isospin density, ρ_I, with the proton/neutron densities:

$$\rho_{P,N} = \tfrac{1}{2}\rho \pm \rho_I, \tag{5.1}$$

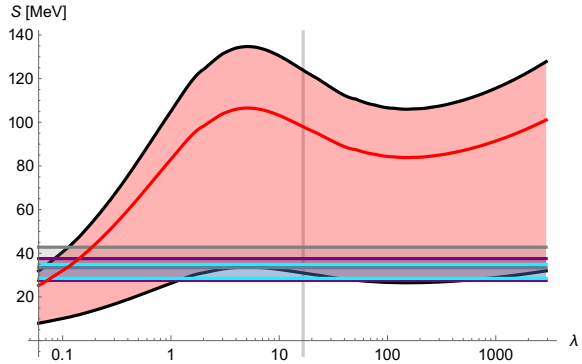

Figure 2. The symmetry energy (SE) calculated in the WSS model using quantization of isospin as a function of the 't Hooft coupling λ at saturation density. The red area spans the mass scale $M_{\rm KK}$ from 300MeV to 1200MeV and the red line is at 949MeV. The gray, cyan and purple shaded areas are the same as in Fig. 1. The vertical gray line marks the phenomenological 't Hooft coupling $\lambda = 16.63$ [19].

where the upper sign is for protons and the lower for neutrons. Charge neutrality is imposed by

$$\tfrac{1}{2}\rho + \rho_I = \textstyle\sum_\ell \rho_\ell, \tag{5.2}$$

with $\ell = e, \mu$ being a sum over the charged leptons and the β-equilibrium (from the decay $N \to P + \ell + \bar{\nu}_\ell$) amounts to

$$\mu_\ell = \mu_N - \mu_P = -\mu_I, \qquad \ell = e, \mu, \tag{5.3}$$

where μ_X is the chemical potential of the particle species X. The lepton density is calculated assuming it to be a (massive) Fermi gas as [35]

$$\rho_\ell = \Theta_H(\mu_\ell - m_\ell)\frac{(\mu_\ell^2 - m_\ell^2)^{\frac{3}{2}}}{3\pi^2}, \tag{5.4}$$

with Θ_H being the Heaviside step function, μ_ℓ the chemical potential and m_ℓ being the mass of the lepton ℓ. Using the definition of the isospin chemical potential as being the conjugate variable of the isospin density, we get

$$\mu_I = \frac{1}{V}\frac{\partial H}{\partial \rho_I} = \frac{\rho_I}{\Lambda(\rho)}. \tag{5.5}$$

Inserting eq. (5.4) into the charge neutrality condition (5.2) and using the β-equilibrium condition (5.3), we obtain an implicit solution for the isospin density, ρ_I, as a function of the density ρ:

$$\frac{\rho_I^3}{3\pi^2\Lambda^3}\left[\Theta_H(-\rho_I) + (1 - R^{-2}m_\mu^2)^{\frac{3}{2}}\Theta_H(-R - m_\mu)\right] + \rho_I + \frac{1}{2}\rho = 0, \qquad R = \frac{\rho_I}{\Lambda}, \tag{5.6}$$

where we have set the electron mass to zero and the dimensionless muon mass parameter is the ratio of the physical mass (105.7MeV) to the mass scale $M_{\rm KK}$ and L^{-1}, for the WSS and the HW models, respectively.

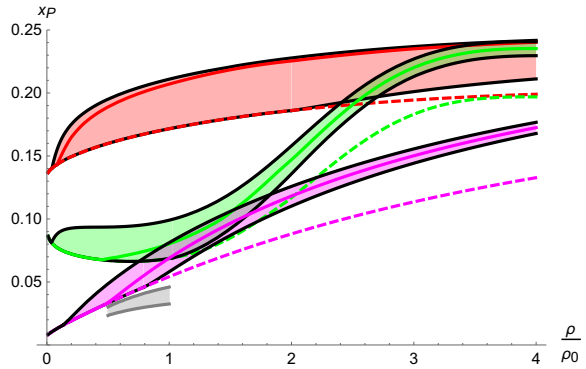

Figure 3. The proton fraction calculated in the WSS and HW model as functions of the density. The red shaded area corresponds to the WSS model with the phenomenological 't Hooft coupling $\lambda = 16.63$ and $M_{\rm KK} \in [300, 1200]$MeV, the red line at $M_{\rm KK} = 949$MeV and the red dashed line at $M_{\rm KK} \to 0$. The green shaded area corresponds to the HW model with $\mathsf{L}^{-1} \in [110, 320]$MeV, the green line at $\mathsf{L}^{-1} = 150$MeV and the green dashed line is the limit $\mathsf{L}^{-1} \to 0$. The magenta shaded area corresponds to the WSS model with the calibration of Fig. 1b), i.e. $\lambda = 60$ and $M_{\rm KK} \in [370, 949]$MeV, the solid magenta curve corresponds to the phenomenological pion decay constant, and the dashed magenta curve corresponds to $M_{\rm KK} \to 0$, thus eliminating the muons. The gray shaded area is the result from chiral EFT [50].

In Fig. 3 we show the numerical results for both the WSS and the HW model for the proton fraction at various densities around saturation density. We find that the HW model gives more realistic proton fractions (green shaded area) than the WSS model fitted phenomenologically to mesons (red shaded area), but yields quite good proton fractions below saturation density if we use the calibration from Fig. 1b), i.e. $\lambda = 60$ and $M_{\rm KK} = 370$MeV. Since we take the electrons to be massless, the mass scale of the model only enters in the muon mass parameter. The dashed curves correspond to the muon being infinitely heavy (or the mass scale of the model being sent to zero).

6 Discussion

In this paper, we have computed the symmetry energy in two holographic QCD models using the method of quantizing the isospin symmetry, namely in the top-down WSS model and the bottom-up HW model. We find fairly good agreement between our model results for the SE and proton fraction in both the HW model, using the fit from neutron stars and in the WSS model with a new calibration.

We have also shown that the method known from Skyrmions of quantizing the isospin zeromode is equivalent to introducing a chemical potential on the holographic boundary for the gauge fields.

It would be interesting in future work to take into account the strange quark (3 instead of 2 flavors) or alternatively the kaons, to see at what densities it might have an impact on the SE. Furthermore, there are certain transitions that happen at larger densities, for example the Skyrmion-half-Skyrmion transition [51], which has an analog in holographic instantons [52]. Although it is not directly observable in our homogeneous Ansatz, it may

have some effect on the SE and proton fractions at large densities. The holographic popcorn transition that is known to occur in HQCD [53, 37] is already taken into account in our models and has observable consequences for the SE, especially the $K_{\rm sym}$ becomes positive in the HW model due to an earlier (wrt. WSS) appearance of the transition – better future experimental constraints may help to pinpoint the best HQCD model for finite density calculations.

Acknowledgments

We thank Nicolas Kovensky, Anton Rebhan and Andreas Schmitt for discussions and comments on the draft. The work of L. B. is supported by the National Natural Science Foundation of China (Grant No. 12150410316). S. B. G. thanks the Outstanding Talent Program of Henan University and the Ministry of Education of Henan Province for partial support. The work of S. B. G. is supported by the National Natural Science Foundation of China (Grants No. 11675223 and No. 12071111) and by the Ministry of Science and Technology of China (Grant No. G2022026021L).

A Equivalence between rotation in SU(2) and external isospin chemical potential

We start with our field configuration given by eq. (3.18), of which we rewrite the non Abelian components:

$$A_0 = Ga\boldsymbol{\chi}\cdot\boldsymbol{\tau}a^{-1} \tag{A.1}$$

$$A_i = -\frac{H}{2}a\tau^i a^{-1}, \tag{A.2}$$

$$A_z = 0. \tag{A.3}$$

We now perform a gauge transformation, with the aim of obtaining a static configuration in the limit of constant $\boldsymbol{\chi}$: we choose a gauge function $b(t)$ that only depends on time, so that the fields transform as

$$A_0 \to \widetilde{A}_0 = Gba\boldsymbol{\chi}\cdot\boldsymbol{\tau}a^{-1}b^{-1} - \mathrm{i}b\partial_0 b^{-1}, \tag{A.4}$$

$$A_i \to \widetilde{A}_i = -\frac{H}{2}ba\tau^i a^{-1}b^{-1}, \tag{A.5}$$

$$A_z \to \widetilde{A}_z = 0. \tag{A.6}$$

Now we choose $b = a^{-1}$, hence rotating the fields A_i back to the standard orientation, while modifying the field A_0 with an additional term:

$$\widetilde{A}_0 = G\boldsymbol{\chi}\cdot\boldsymbol{\tau} - \mathrm{i}a^{-1}\dot{a} \tag{A.7}$$

$$\widetilde{A}_i = -\frac{H}{2}\tau^i, \tag{A.8}$$

$$\widetilde{A}_z = 0. \tag{A.9}$$

We recognize the quantity of eq. (3.10) in the last term of eq. (A.7):

$$-\mathrm{i}a^{-1}\dot{a} = \frac{1}{2}\boldsymbol{\chi}\cdot\boldsymbol{\tau}, \tag{A.10}$$

so that we are left with

$$\widetilde{A}_0 = \left(G + \frac{1}{2}\right) \boldsymbol{\chi} \cdot \boldsymbol{\tau}. \tag{A.11}$$

We know that by construction the function $G(z)$ vanishes at the boundary at $z_{\rm UV}$, so we conclude that this configuration behaves as:

$$\widetilde{A}_0(z \to z_{\rm UV}) = \frac{1}{2} \boldsymbol{\chi} \cdot \boldsymbol{\tau}. \tag{A.12}$$

The boundary value of the field A_0 is dual to an isospin chemical potential in the holographic dictionary. Since the orientation of the soliton is a zeromode, we can set $\boldsymbol{\chi}$ to point in a chosen direction for simplicity without loss of generality: we choose it to have only a nonvanishing third component as $\boldsymbol{\chi} = (0, 0, \mu_I)$, following the same convention of choosing the third component of isospin as the operator to diagonalize simultaneously with the isospin squared (and the isospin chemical potential to appear holographically as the boundary value of $A_0^{a=3}$). Shifting $G(z)$ as

$$\widetilde{G}(z) = \left(G(z) + \frac{1}{2}\right), \tag{A.13}$$

we obtain the familiar expressions for the gauge field and its boundary condition

$$\widetilde{A}_0 = \widetilde{G} \tau^3 \mu_I, \qquad \widetilde{A}_0(z \to z_{\rm UV}) = \frac{1}{2} \mu_I \tau^3. \tag{A.14}$$

We then conclude that a static system in the presence of an external isospin chemical potential μ_I is equivalently described as it rotating in isospin space with angular velocity $\chi^i = \mu_I \delta^{i3}$, as observed in ref. [54] in the non-holographic context of the Skyrme model.

We want to emphasize that, despite our solution to the system of coupled equations of motion is performed in the limit of small angular velocity (small μ_I), the equivalence between the two methods just shown holds true in general, since we made no assumptions on the χ dependence of the functions $H, \widehat{a}_0, G, L$. The assumption of small χ will not affect in any way the calculation of the symmetry energy, as it is the coefficient of a term of an expansion around symmetric matter, hence all the functions would have to be evaluated at vanishing isospin density (and μ_I) anyway.

B Isospin density from holographic current

In this section we want to prove that the isospin number density that we defined from the quantized angular momentum coincides with the canonical one obtained through the holographic dictionary via the computation of the isovectorial current. For simplicity, we will show the proof in the WSS model, so that $z_{\rm IR} = 0$, $z_{\rm UV} = +\infty$, but it holds true in the HW model too, after substitution of the appropriate quantities. As shown in ref. [39], the vectorial current is obtained as

$$\mathcal{J}_{V\mu} = -\kappa \left[k(z) \mathcal{F}_{\mu z}\right]_{-\infty}^{+\infty} = -2\kappa \left[k(z) \mathcal{F}_{\mu z}\right]_{0}^{+\infty}. \tag{B.1}$$

With this quantity we can build the isovectorial charge Q_V of which we take the third component to coincide with the isospin operator

$$Q_V^{a=3} = I_3 = \int d^3x \, \mathrm{Tr}\left(J_V^0 \tau^3\right) = V \, \mathrm{Tr}\left(J_V^0 \tau^3\right). \tag{B.2}$$

We plug in this formula the homogeneous Ansatz (3.18):

$$I_3 = -2\kappa V \left[G' k(z)\right]_0^{+\infty} \chi^i \, \mathrm{Tr}\left(a\tau^i a^{-1} \tau^3\right) = \tag{B.3}$$

$$= -2\kappa V \left[G' k(z)\right]_{z=+\infty} \chi^i \, \mathrm{Tr}\left(a\tau^i a^{-1} \tau^3\right), \tag{B.4}$$

where we used the fact that $G'(0) = 0$.

The angular velocity χ^i is related to the angular momentum operator J^i by the familiar relation involving the moment of inertia Λ:

$$\chi^i = \frac{1}{V\Lambda} J^i, \tag{B.5}$$

and we can exploit the useful relationship between angular momentum and isospin operators that holds due to the spherical symmetry of the system:

$$J^i \, \mathrm{Tr}\left(a\tau^i a^{-1} \tau^a\right) = -2I_a, \tag{B.6}$$

so that we are left with:

$$I_3 = \frac{4\kappa}{\Lambda} \left[G' k(z)\right]_{z=+\infty} I_3. \tag{B.7}$$

We see that the validity of this relationship depends on wether the following identification holds true:

$$4\kappa \left[G' k(z)\right]_{z=+\infty} = \Lambda. \tag{B.8}$$

To prove this relationship, we first notice that the formula for the current is obtained by differentiating the action with respect to the UV boundary value of the A_0 field, following

$$\delta_{A_0} S = (\text{e.o.m. terms}) + 4\kappa V \, \mathrm{Tr}\left[k(z) A_0' \delta A_0\right]_{z=+\infty}, \tag{B.9}$$

where the first term means that we neglect contributions that vanish by the equations of motion, we evaluate only boundary terms, and we made use of the boundary condition $A_0'(z=0) = 0$. We decide to employ the gauge in which the field A_0 has a finite boundary value, dual to the isospin chemical potential, so we take the field to be as in eq. (A.14). With this configuration, the variation of the action assumes the shape

$$\delta_{A_0} S = (\text{e.o.m. terms}) + 2\kappa V \, \mathrm{Tr}\left[k(z) \widetilde{G}' \tau^3 \tau^3\right]_{z=+\infty} \mu_I \delta\mu_I, \tag{B.10}$$

and finally we can compute the derivative

$$\frac{\partial S}{\partial \mu_I} = 4\kappa V \left[k(z) \widetilde{G}'\right]_{z=+\infty} \mu_I. \tag{B.11}$$

We can change this result to our usual "rotating" gauge by noting that we have to rename $\mu_I \to \chi_3$, and that $\widetilde{G}' = G'$, so that on-shell we obtain

$$\frac{\partial S}{\partial \chi_3} = 4\kappa V \left[k(z)G'\right]_{z=+\infty} \chi_3. \tag{B.12}$$

We now look at the definition of Λ: it is nothing but the part of the energy density that is quadratic in the angular velocity, and there is no linear term. In this picture, the system is rotating and there is no chemical potential, so the on-shell action gives the energy of the system, so that we can write

$$\frac{\partial S}{\partial \chi_3} = V\Lambda\chi_3. \tag{B.13}$$

Comparing eqs. (B.11) and (B.13), we finally prove eq. (B.8).

References

[1] M. Baldo, G. F. Burgio, The nuclear symmetry energy, Prog. Part. Nucl. Phys. 91 (2016) 203–258. arXiv:1606.08838, doi:10.1016/j.ppnp.2016.06.006.

[2] P. Danielewicz, J. Lee, Symmetry Energy II: Isobaric Analog States, Nucl. Phys. A 922 (2014) 1–70. arXiv:1307.4130, doi:10.1016/j.nuclphysa.2013.11.005.

[3] G. Fiorella Burgio, A. F. Fantina, Nuclear Equation of state for Compact Stars and Supernovae, Astrophys. Space Sci. Libr. 457 (2018) 255–335. arXiv:1804.03020, doi:10.1007/978-3-319-97616-7_6.

[4] B.-A. Li, B.-J. Cai, W.-J. Xie, N.-B. Zhang, Progress in Constraining Nuclear Symmetry Energy Using Neutron Star Observables Since GW170817, Universe 7 (6) (2021) 182. arXiv:2105.04629, doi:10.3390/universe7060182.

[5] S.-P. Tang, J.-L. Jiang, M.-Z. Han, Y.-Z. Fan, D.-M. Wei, Constraints on the phase transition and nuclear symmetry parameters from PSR J0740+6620 and multimessenger data of other neutron stars, Phys. Rev. D 104 (6) (2021) 063032. arXiv:2106.04204, doi:10.1103/PhysRevD.104.063032.

[6] B. T. Reed, F. J. Fattoyev, C. J. Horowitz, J. Piekarewicz, Implications of PREX-2 on the Equation of State of Neutron-Rich Matter, Phys. Rev. Lett. 126 (17) (2021) 172503. arXiv:2101.03193, doi:10.1103/PhysRevLett.126.172503.

[7] R. Essick, P. Landry, A. Schwenk, I. Tews, Detailed examination of astrophysical constraints on the symmetry energy and the neutron skin of Pb208 with minimal modeling assumptions, Phys. Rev. C 104 (6) (2021) 065804. arXiv:2107.05528, doi:10.1103/PhysRevC.104.065804.

[8] H. Gil, P. Papakonstantinou, C. H. Hyun, Constraints on the curvature of nuclear symmetry energy from recent astronomical data within the KIDS framework, Int. J. Mod. Phys. E 31 (01) (2022) 2250013. arXiv:2110.09802, doi:10.1142/S0218301322500136.

[9] P. B. de Tovar, M. Ferreira, C. Providência, Determination of the symmetry energy from the neutron star equation of state, Phys. Rev. D 104 (12) (2021) 123036. arXiv:2112.05551, doi:10.1103/PhysRevD.104.123036.

[10] B. R. Barrett, P. Navratil, J. P. Vary, Ab initio no core shell model, Prog. Part. Nucl. Phys. 69 (2013) 131–181. doi:10.1016/j.ppnp.2012.10.003.

[11] I. Tews, T. Krüger, K. Hebeler, A. Schwenk, Neutron matter at next-to-next-to-next-to-leading order in chiral effective field theory, Phys. Rev. Lett. 110 (3) (2013) 032504. arXiv:1206.0025, doi:10.1103/PhysRevLett.110.032504.

[12] A. Kurkela, P. Romatschke, A. Vuorinen, Cold Quark Matter, Phys. Rev. D 81 (2010) 105021. arXiv:0912.1856, doi:10.1103/PhysRevD.81.105021.

[13] J. M. Maldacena, The Large N limit of superconformal field theories and supergravity, Adv. Theor. Math. Phys. 2 (1998) 231–252. arXiv:hep-th/9711200, doi:10.1023/A:1026654312961.

[14] E. Witten, Anti-de Sitter space, thermal phase transition, and confinement in gauge theories, Adv. Theor. Math. Phys. 2 (1998) 505–532. arXiv:hep-th/9803131, doi:10.4310/ATMP.1998.v2.n3.a3.

[15] Y. Kim, I. J. Shin, T. Tsukioka, Holographic QCD: Past, Present, and Future, Prog. Part. Nucl. Phys. 68 (2013) 55–112. arXiv:1205.4852, doi:10.1016/j.ppnp.2012.09.002.

[16] A. Rebhan, The Witten-Sakai-Sugimoto model: A brief review and some recent results, EPJ Web Conf. 95 (2015) 02005. arXiv:1410.8858, doi:10.1051/epjconf/20159502005.

[17] M. Ammon, J. Erdmenger, Gauge/gravity duality: Foundations and applications, Cambridge University Press, Cambridge, 2015.

[18] T. Sakai, S. Sugimoto, Low energy hadron physics in holographic QCD, Prog. Theor. Phys. 113 (2005) 843–882. arXiv:hep-th/0412141, doi:10.1143/PTP.113.843.

[19] T. Sakai, S. Sugimoto, More on a holographic dual of QCD, Prog. Theor. Phys. 114 (2005) 1083–1118. arXiv:hep-th/0507073, doi:10.1143/PTP.114.1083.

[20] U. Gursoy, E. Kiritsis, Exploring improved holographic theories for QCD: Part I, JHEP 02 (2008) 032. arXiv:0707.1324, doi:10.1088/1126-6708/2008/02/032.

[21] U. Gursoy, E. Kiritsis, F. Nitti, Exploring improved holographic theories for QCD: Part II, JHEP 02 (2008) 019. arXiv:0707.1349, doi:10.1088/1126-6708/2008/02/019.

[22] M. Jarvinen, E. Kiritsis, Holographic Models for QCD in the Veneziano Limit, JHEP 03 (2012) 002. arXiv:1112.1261, doi:10.1007/JHEP03(2012)002.

[23] T. Alho, M. Järvinen, K. Kajantie, E. Kiritsis, C. Rosen, K. Tuominen, A holographic model for QCD in the Veneziano limit at finite temperature and density, JHEP 04 (2014) 124, [Erratum: JHEP 02, 033 (2015)]. arXiv:1312.5199, doi:10.1007/JHEP04(2014)124.

[24] M. Järvinen, Holographic modeling of nuclear matter and neutron stars, Eur. Phys. J. C 82 (4) (2022) 282. arXiv:2110.08281, doi:10.1140/epjc/s10052-022-10227-x.

[25] J. Polchinski, M. J. Strassler, Hard scattering and gauge/string duality, Phys. Rev. Lett. 88 (2002) 031601. arXiv:hep-th/0109174, doi:10.1103/PhysRevLett.88.031601.

[26] H. Boschi-Filho, N. R. F. Braga, QCD/string holographic mapping and glueball mass spectrum, Eur. Phys. J. C 32 (2004) 529–533. arXiv:hep-th/0209080, doi:10.1140/epjc/s2003-01526-4.

[27] J. Polchinski, M. J. Strassler, Deep inelastic scattering and gauge/string duality, JHEP 05 (2003) 012. arXiv:hep-th/0209211, doi:10.1088/1126-6708/2003/05/012.

[28] H. Boschi-Filho, N. R. F. Braga, Gauge/string duality and scalar glueball mass ratios, JHEP 05 (2003) 009. arXiv:hep-th/0212207, doi:10.1088/1126-6708/2003/05/009.

[29] G. F. de Teramond, S. J. Brodsky, Hadronic spectrum of a holographic dual of QCD, Phys.

Rev. Lett. 94 (2005) 201601. arXiv:hep-th/0501022, doi:10.1103/PhysRevLett.94.201601.

[30] J. Erlich, E. Katz, D. T. Son, M. A. Stephanov, QCD and a holographic model of hadrons, Phys. Rev. Lett. 95 (2005) 261602. arXiv:hep-ph/0501128, doi:10.1103/PhysRevLett.95.261602.

[31] L. Da Rold, A. Pomarol, The Scalar and pseudoscalar sector in a five-dimensional approach to chiral symmetry breaking, JHEP 01 (2006) 157. arXiv:hep-ph/0510268, doi:10.1088/1126-6708/2006/01/157.

[32] J. Hirn, V. Sanz, Interpolating between low and high energy QCD via a 5-D Yang-Mills model, JHEP 12 (2005) 030. arXiv:hep-ph/0507049, doi:10.1088/1126-6708/2005/12/030.

[33] A. Karch, E. Katz, D. T. Son, M. A. Stephanov, Linear confinement and AdS/QCD, Phys. Rev. D 74 (2006) 015005. arXiv:hep-ph/0602229, doi:10.1103/PhysRevD.74.015005.

[34] Y. Kim, Y. Seo, I. J. Shin, S.-J. Sin, Symmetry energy of dense matter in holographic QCD, JHEP 06 (2011) 011. arXiv:1011.0868, doi:10.1007/JHEP06(2011)011.

[35] N. Kovensky, A. Schmitt, Isospin asymmetry in holographic baryonic matter, SciPost Phys. 11 (2) (2021) 029. arXiv:2105.03218, doi:10.21468/SciPostPhys.11.2.029.

[36] N. Kovensky, A. Poole, A. Schmitt, Building a realistic neutron star from holography, Phys. Rev. D 105 (3) (2022) 034022. arXiv:2111.03374, doi:10.1103/PhysRevD.105.034022.

[37] L. Bartolini, S. B. Gudnason, J. Leutgeb, A. Rebhan, Neutron stars and phase diagram in a hard-wall AdS/QCD model, Phys. Rev. D 105 (12) (2022) 126014. arXiv:2202.12845, doi:10.1103/PhysRevD.105.126014.

[38] H. Hata, T. Sakai, S. Sugimoto, S. Yamato, Baryons from instantons in holographic QCD, Prog. Theor. Phys. 117 (2007) 1157. arXiv:hep-th/0701280, doi:10.1143/PTP.117.1157.

[39] K. Hashimoto, T. Sakai, S. Sugimoto, Holographic Baryons: Static Properties and Form Factors from Gauge/String Duality, Prog. Theor. Phys. 120 (2008) 1093–1137. arXiv:0806.3122, doi:10.1143/PTP.120.1093.

[40] S. Bolognesi, P. Sutcliffe, The Sakai-Sugimoto soliton, JHEP 01 (2014) 078. arXiv:1309.1396, doi:10.1007/JHEP01(2014)078.

[41] G. S. Adkins, C. R. Nappi, E. Witten, Static Properties of Nucleons in the Skyrme Model, Nucl. Phys. B 228 (1983) 552. doi:10.1016/0550-3213(83)90559-X.

[42] H. K. Lee, B.-Y. Park, M. Rho, Half-Skyrmions, Tensor Forces and Symmetry Energy in Cold Dense Matter, Phys. Rev. C 83 (2011) 025206, [Erratum: Phys.Rev.C 84, 059902 (2011)]. arXiv:1005.0255, doi:10.1103/PhysRevC.84.059902.

[43] C. Adam, A. Garcia Martin-Caro, M. Huidobro, R. Vázquez, A. Wereszczynski, Quantum skyrmion crystals and the symmetry energy of dense matter, Phys. Rev. D 106 (11) (2022) 114031. arXiv:2202.00953, doi:10.1103/PhysRevD.106.114031.

[44] F. Bigazzi, P. Niro, Neutron-proton mass difference from gauge/gravity duality, Phys. Rev. D 98 (4) (2018) 046004. arXiv:1803.05202, doi:10.1103/PhysRevD.98.046004.

[45] J. Cruz Rojas, T. Demircik, M. Järvinen, Popcorn Transitions and Approach to Conformality in Homogeneous Holographic Nuclear Matter, Symmetry 15 (2) (2023) 331. arXiv:2301.03173, doi:10.3390/sym15020331.

[46] N. Kovensky, A. Poole, A. Schmitt, Phases of cold holographic QCD: baryons, pions and rho

mesons (2 2023). arXiv:2302.10675.

[47] A. Ilderton, Radial evolution in anti-de Sitter spacetime, Int. J. Mod. Phys. A 21 (2006) 3289–3294. arXiv:hep-th/0501218, doi:10.1142/S0217751X06031338.

[48] S. Baldino, S. Bolognesi, S. B. Gudnason, D. Koksal, Solitonic approach to holographic nuclear physics, Phys. Rev. D 96 (3) (2017) 034008. arXiv:1703.08695, doi:10.1103/PhysRevD.96.034008.

[49] S. Baldino, L. Bartolini, S. Bolognesi, S. B. Gudnason, Holographic Nuclear Physics with Massive Quarks, Phys. Rev. D 103 (12) (2021) 126015. arXiv:2102.00680, doi:10.1103/PhysRevD.103.126015.

[50] Y. Lim, J. W. Holt, Proton pairing in neutron stars from chiral effective field theory, Phys. Rev. C 103 (2) (2021) 025807. arXiv:1709.08793, doi:10.1103/PhysRevC.103.025807.

[51] B.-Y. Park, J.-I. Kim, M. Rho, Kaons in Dense Half-Skyrmion Matter, Phys. Rev. C 81 (2010) 035203. arXiv:0912.3213, doi:10.1103/PhysRevC.81.035203.

[52] M. Rho, S.-J. Sin, I. Zahed, Dense QCD: A Holographic Dyonic Salt, Phys. Lett. B 689 (2010) 23–27. arXiv:0910.3774, doi:10.1016/j.physletb.2010.01.077.

[53] V. Kaplunovsky, D. Melnikov, J. Sonnenschein, Baryonic Popcorn, JHEP 11 (2012) 047. arXiv:1201.1331, doi:10.1007/JHEP11(2012)047.

[54] C. Adam, A. Garcia Martin-Caro, M. Huidobro, A. Wereszczynski, Skyrme Crystals, Nuclear Matter and Compact Stars, Symmetry 15 (4) (2023) 899. arXiv:2305.06639, doi:10.3390/sym15040899.